J. Chem. Sci. Vol. 123, No. 3, May 2011, pp. 299–309. © Indian Academy of Sciences.

DFT study of the reactions of Mo and Mo^+ with CO_2 in gas phase

DEMAN HAN, GUOLIANG DAI*, HAO CHEN, HUA YAN, JUNYONG WU, CHUANFENG WANG and AIGUO ZHONG

School of Pharmaceutical and Chemical Engineering, Taizhou University, Linhai 317000, People's Republic of China
e-mail: daigl@tzc.edu.cn

MS received 8 April 2010; revised 6 September 2010; accepted 4 February 2011

Abstract. Density functional theory (DFT) calculations have been performed to explore the potential energy surfaces of C–O bond activation in CO_2 molecule by gas-phase Mo^+ cation and Mo atom, in order to better understanding the mechanism of second-row metal reacting with CO_2. The minimum energy reaction path is found to involve the spin inversion in the different reaction steps. This potential energy curve-crossing dramatically affects reaction exothermic. The present results show that the reaction mechanism is insertion-elimination mechanism along the C–O bond activation branch. All the theoretical results not only support the existing conclusions inferred from early experiment, but also complement the pathway and mechanism for this reaction.

Keywords. Density functional theory; potential energy surface; transition-metal; reaction mechanism.

1. Introduction

Carbon dioxide is a main contributor to global warming. How to remove this long-lived greenhouse gas from industrial emission and to recycle it have become one of the most challenging subjects nowadays.[1] As it is difficult to reduce significantly CO_2 emissions from anthropic sources, in the past many years, considerable attention has been paid to convert this species into more useful chemical materials due to its abundance and renewablility. But new ways must be found to activate the molecule if its potential has to be realized. Activation is one of the effective routes to induce inert molecules to react. In previous years, many types of metal and metal oxide were used as catalysts to activate CO_2, and much interest has been focused on the experimental and theoretical studies of transition metal-CO_2 complexes,[2–41] as such complexes have potential for practical application in activating CO_2.

As a representative of the second-row transition metal, molybdenum is effective in activating some important moleculars such as CO_2,[18,40] CH_4,[42] C_3H_8,[43,44] O_2 [45] Sievers *et al.*[40] have examined the reaction of Mo^+ with CO_2, where metal-oxygen bond energies were determined. In this reaction, MoO^+ is found to be the dominant product at low energy condition. Based on the experiment, they also investigated the gas-phase carbon dioxide activation by Mo^+ cation at the density functional level of theory and brought out that the CO_2 activation mediated by Mo^+ cation is a spin-forbidden process which resulted from a crossing between different energetic profiles. But they did not locate the exact region of curve-crossing which may dramatically affect reaction mechanism. Andrews *et al.*[18] performed an IR study on the reaction of laser-ablated Mo atom with CO_2, and reported the observed IR absorptions of the insertion products OMoCO. But to the best of our knowledge, the detailed information for the potential energy surfaces of reactions Mo^++CO_2 and Mo+CO_2 are still scarce. Can a similar reaction mechanism be applicable to the reactions of Mo^+ cation and Mo atom with CO_2? What are the different behaviours between them? Promted by these questions, we investigated the reactions of Mo^+ cation and Mo atom with CO_2 by using DFT methods in detail in order to shed some light on these reactions. A comparative theoretical study on the reactions of Mo^+ cation and Mo atom with CO_2 is interesting and important since molybdenum is a representative of the second-row transition metal.

2. Computational methods

The sextet, quartet and doublet PESs for the reaction of $Mo^+ + CO_2$ and the quintet, triplet and singlet

*For correspondence

PESs for the reaction of Mo + CO_2 have been considered in detail. We optimized all molecular geometries (reactants, intermediates, transition states and products) by employing the B3LYP density functional theory method.[46,47] The spin-unrestricted version of this methodology was used for the calculations of doublet, triplet, quartet, quintet and sextet PESs. As for the singlet PES, we used the RB3LYP density functional theory method. These methods are chosen in this study since the previous calibration calculations on transition-metal compounds have shown that this hybrid functional provides accurate results for the geometries and vibrational frequencies of systems containing transition-metal cations.[48,49] Recently, the potential energy surfaces and reaction mechanisms of C_2H_6 and C_3H_8 activation by Mo^+ were theoretically investigated by Armentrout[43,44] at B3LYP/HW/6−311++G (3df,3p) level, and this method gives good results for the reaction system. In addition, using the B3LYP/sdd/6−311++G (3df, 3pd) method, Guo *et al.*[50] also gained good results of CH_4 activation by Molybdenum atoms. In all of our calculations, the 6−311+G(2d) basis set was used for the carbon and oxygen atoms, and the effective core potentials (ECP) of Stuttgart[51] basis set was used for the molybdenum, the 5s and 4d in Mo were treated explicitly by a (8s7p6d) Gaussian basis set contracted to [6s5p3d]. We inspected the values of $<S^2>$ for all species involved in the reaction of Mo and Mo^+ toward CO_2, and found that the deviation of $<S^2>$ is less than 3%, which indicates that the spin contaminations were small in all the calculations. The harmonic vibration analyses were performed at the same level of theory for all optimized stationary points to determine their characters (minimum or first-order saddle point) and to evaluate the zero-point vibrational energies (ZPEs). To verify whether the located transition states connect the expected minima, intrinsic reaction coordinate (IRC) calculations were carried out for each transition state at the same level.[52] All calculations in the present study were performed using the Gaussian 03 program.[53]

3. Results and discussion

The optimized geometries of the stationary points for the reactions of Mo^+ and Mo with CO_2 are depicted in figures 1a and b respectively. The profiles of the PESs are shown in figure 2. The relevant energies of various compounds in the reaction are listed in tables 1 and 2, and the potential energies curve-crossing diagrams between the different potential energy surfaces are drawn in figure 3.

3.1 *The reaction between Mo^+ and CO_2*

The energy of ground state $^6Mo^+$ is lower than that of excited states $^4Mo^+$and $^2Mo^+$ by 32.61 kcal/mol and 60.15 kcal/mol respectively at the chosen level, so the reaction between ground state Mo^+ and CO_2 is more favourable at low energy condition. As for the sextet PES, the reaction starts with the formation of a linear encounter complex ^{6}IM1($^6\Sigma$, $C_{\infty v}$), which is 20.76 kcal/mol below the entrance channel $^6Mo^+$+CO_2. It should be pointed out that although numerous trials are taken to search for possible transition states that connect reactants and original complex, no such structures are obtained. For example, in the case of the formation of this linear encounter complex ^{6}IM1, for a given Mo–O bond length, all other geometrical degrees of freedom are optimized, as Mo approaches the oxygen atom, the energy of the complex decreases monotonically until formation of the encounter complex ^{6}IM1. Clearly, the formation of ^{6}IM1 is spontaneous and it is a barrier-free process. Subsequently, this encounter species proceeds to form the insertion complex ^{6}IM3 through the transition state $^6TS_{13}$. This insertion process is endothermic by 74.85 kcal/mol and has a barrier of 79.81 kcal/mol. These results show that it is much different for ground state $^6Mo^+$ cation to cleave the C–O bond in CO_2. As shown in figure 1a, the Mo–O distance in $^6TS_{13}$ is shortened from 2.277 Å to 1.965 Å, and the Mo–C bond is shortened to 2.141 Å. These facts indicate that the weak electrostatic interaction between Mo^+ and CO_2 has strengthened when it is converted into $^6TS_{13}$. Synchronously, the C–O bond breaks gradually, the bond length is increased by 0.708 Å. $^6TS_{13}$ has a three-member-ring structure with C_s symmetry. The imaginary frequency is 406.9i cm^{-1}, and the normal model corresponds to the rupture of C–O bond and the formation of Mo–O and Mo–C bonds.

As shown in figure 1a, ^{6}IM3 (^{6}A', C_s) is an insertion species of Mo^+ cation into the C–O bond. Compared with the transition state $^6TS_{13}$, the structures of these two species are very similar, and the energy of ^{6}IM3 is only 4.96 kcal/mol more stable. Obviously, $^6TS_{13}$ is a typical late transition state. NBO calculation shows that in ^{6}IM3 two single bonds have formed between Mo and O, Mo and C atoms respectively. The NBO charge on the Mo atom increases to about + 1.306e, whereas the atomic charge on carbon atom decreases to 0.229 e (it is

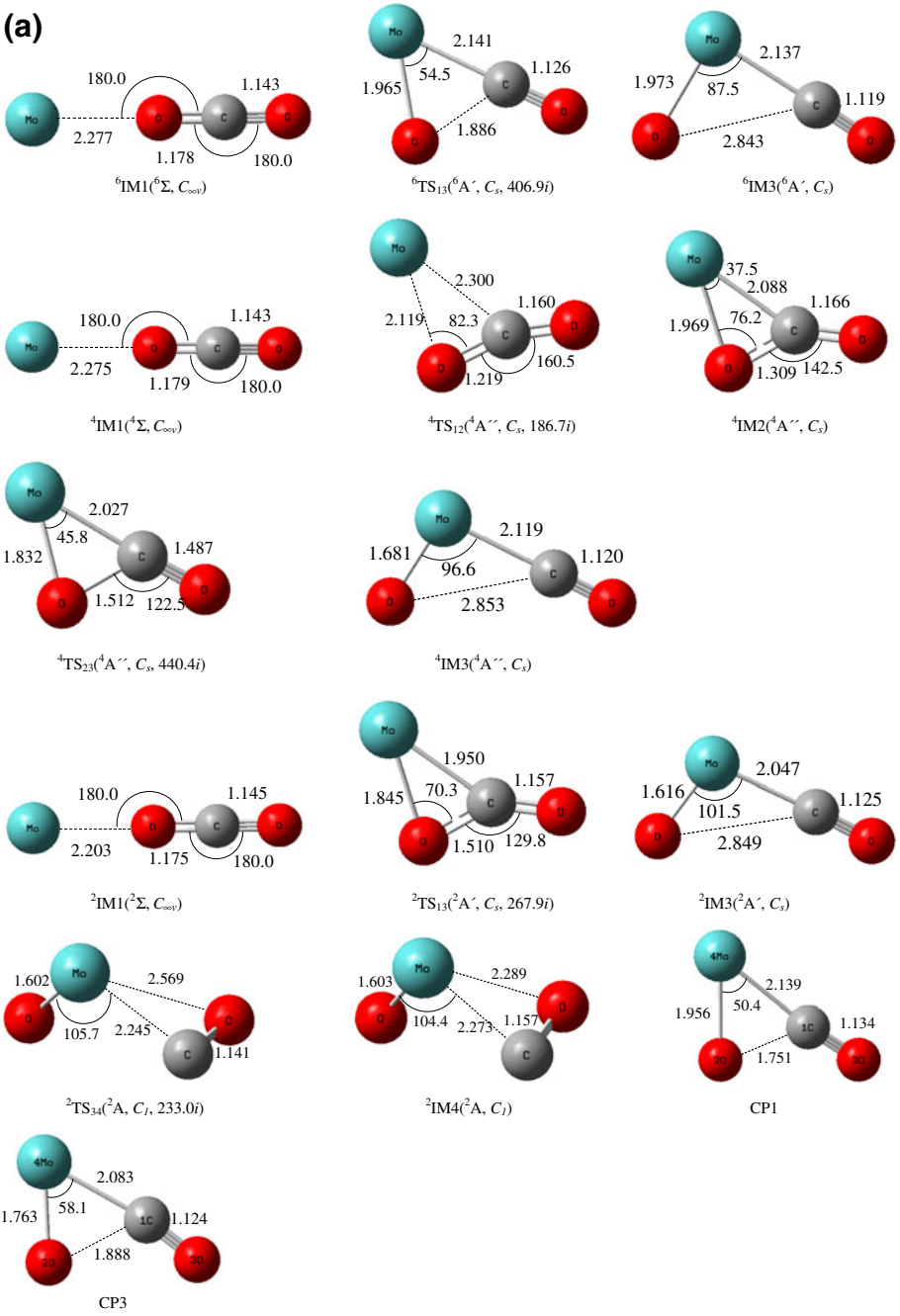

Figure 1. (**a**) Optimized geometries for the various stationary points and crossing points located on the $Mo^+ + CO_2$ potential energy surfaces (distances in angstroms, angles in degrees). (**b**) Optimized geometries for the various stationary points and crossing points located on the Mo + CO_2 potential energy surfaces (distances in angstroms, angles in degrees).

0.997 *e* in free CO_2). The OMo–CO binding energy is 35.84 kcal/mol which can be basically attributed to the Mo–C bond arising from a CO→Mo σ-donation and a simultaneous Mo→CO π-back-donation.

The next step is the non-reactive-dissociation of ^{6}IM3 to generate products. After calculation, we found the insertion species ^{6}IM3 can dissociate directly without exit barrier to products $^6MoO^+$ + CO and $^6MoCO^+ + {}^3O$, endothermic by 35.84 and 43.43 kcal/mol respectively, so the energetically most favourable channel is to form the dissociation products of $^6MoO^+$ + CO through cleavage of Mo–C

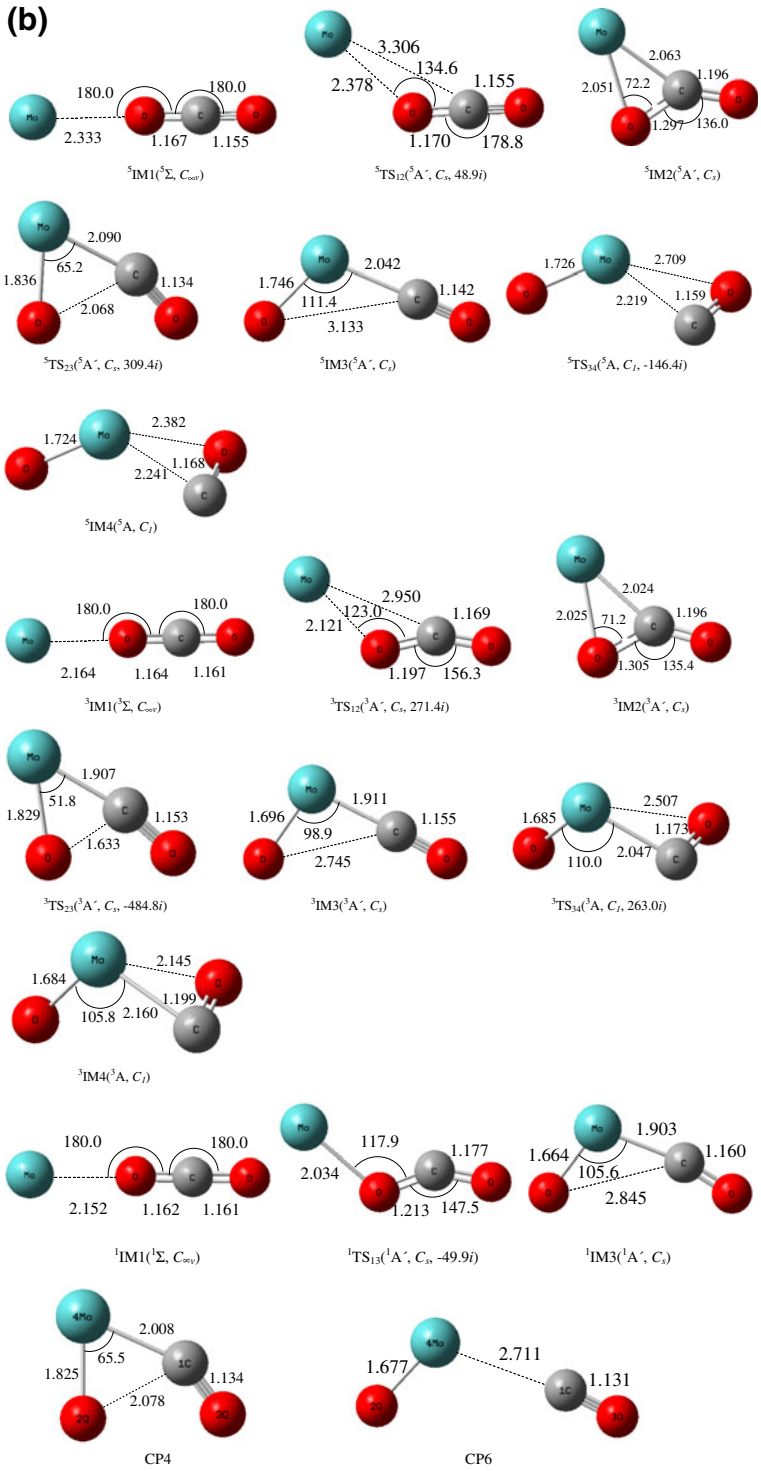

Figure 1. Continued.

bond. It is clear that the reaction mechanism of $^6Mo^+$ with CO_2 over sextet PES is the typical insertion–elimination mechanism.

With respect to the quartet state pathway, the first step of the reaction over this PES starts with the formation of the encounter complex ^{4}IM1 ($^4\Sigma$, $C_{\infty v}$), which is a barrierless process. The relative energy of ^{4}IM1 is calculated to be 29.61 kcal/mol higher than that of the sextet analogue, ^{6}IM1. ^{4}IM1 can convert into a η^2-OC encounter complex ^{4}IM2, with a relatively high activation energy of 36.7 kcal/mol. ^{4}IM2 stores quite high energy, with reaction proceeding, this species may

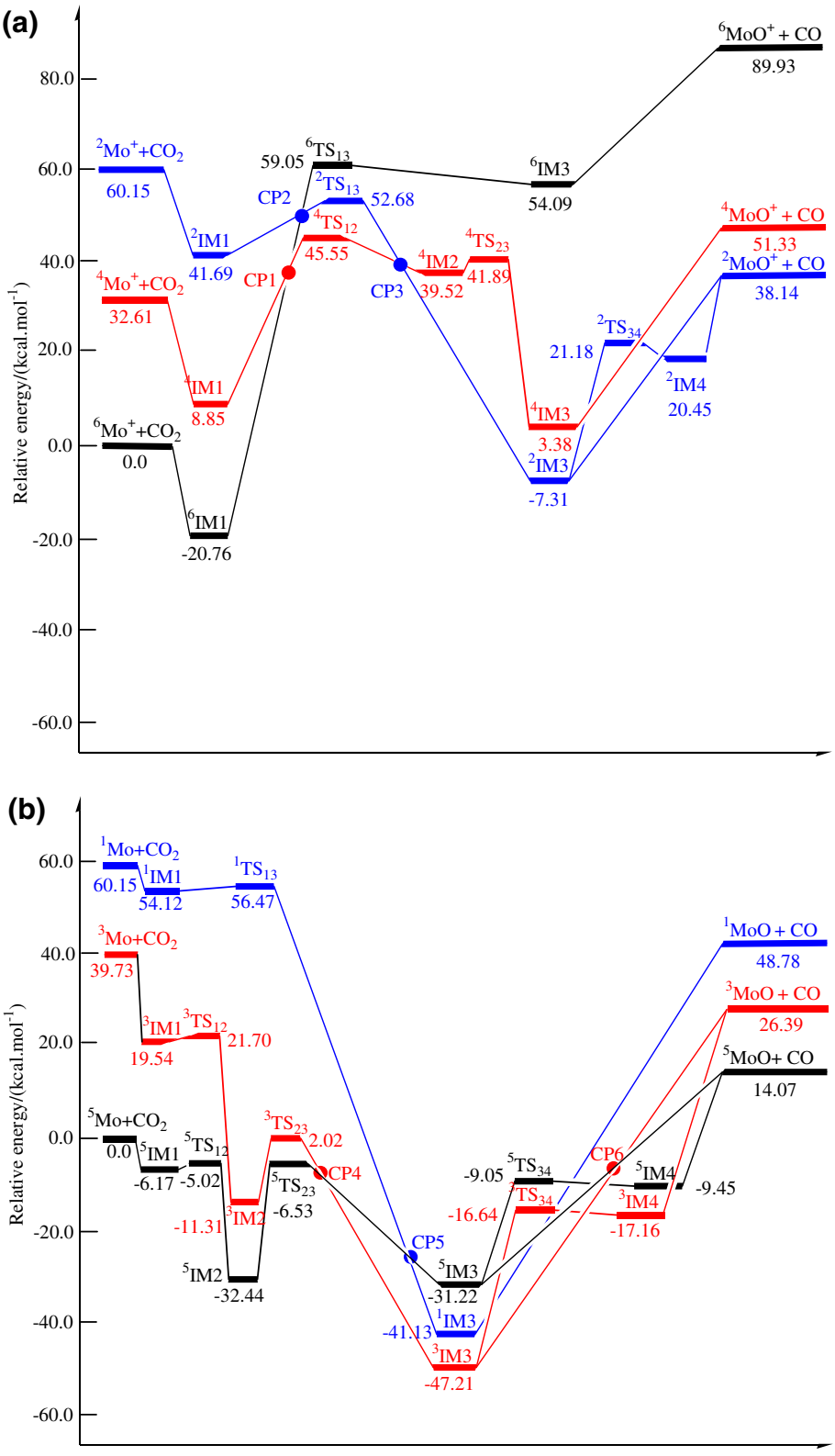

Figure 2. Potential energy surface profiles for the reaction of (**a**) Mo^+ cation with CO_2. (**b**) Mo atom with CO_2.

Table 1. Energy of various complexes in the reaction of Mo^+ cation with CO_2 (total energy E_T, *ZPE* corrections have been taken into account, relative energy E_R).

Species	E_T/Hartree	E_R/ kcal·mol^{-1}	Species	E_T/Hartree	E_R/ kcal·mol^{-1}	Species	E_T/Hartree	E_R/ kcal·mol^{-1}
$^6Mo^+ + CO_2$	−255.472148	0.0	$^4TS_{12}$	−255.399563	45.55	$^2TS_{13}$	−255.388194	52.68
$^6IM1$	−255.505237	−20.76	$^4IM2$	−255.409164	39.52	$^2IM3$	−255.483793	−7.31
$^6TS_{13}$	−255.378046	59.05	$^4TS_{23}$	−255.405398	41.89	$^2TS_{34}$	−255.438397	21.18
$^6IM3$	−255.385954	54.09	$^4IM3$	−255.466755	3.38	$^2IM4$	−255.439558	20.45
$^6MoO^+ + CO$	−255.32884	89.93	$^4MoO^+ + CO$	−255.390351	51.55	$^2MoO^+ + CO$	−255.411365	38.14
$^6MoCO^+ + {}^3O$	−255.316738	97.52	$^4MoCO^+ + {}^3O$	−255.28987	114.38	$^2MoCO^+ + {}^1O$	−255.157591	197.39
$^4Mo^+ + CO_2$	−255.420183	32.61	$^2Mo^+ + CO_2$	−255.376293	60.15			
$^4IM1$	−255.458038	8.85	$^2IM1$	−255.405708	41.69			

Table 2. Energy of various complexes in the reaction of Mo atom with CO_2 (total energy E_T, *ZPE* corrections have been taken into account, relative energy E_R).

Species	E_T/Hartree	E_R/ kcal·mol^{-1}	Species	E_T/Hartree	E_R/ kcal·mol^{-1}	Species	E_T/Hartree	E_R/ kcal·mol^{-1}
$^5Mo + CO_2$	−255.690863	0.0	$^5MoCO + {}^3O$	−255.564516	79.28	$^3MoO + CO$	−255.648813	26.39
$^5IM1$	−255.700694	−6.17	$^3Mo + CO_2$	−255.627557	39.73	$^3MoCO + {}^3O$	−255.536336	96.97
$^5TS_{12}$	−255.698868	−5.02	$^3IM1$	−255.659718	19.54	$^1Mo + CO_2$	−255.573702	73.52
$^5IM2$	−255.740629	−31.22	$^3TS_{12}$	−255.656285	21.70	$^1IM1$	−255.604620	54.12
$^5TS_{23}$	−255.701270	−6.53	$^3IM2$	−255.708890	−11.31	$^1TS_{13}$	−255.600878	56.47
$^5IM3$	−255.742557	−32.44	$^3TS_{23}$	−255.687641	2.02	$^1IM3$	−255.756402	−41.13
$^5TS_{34}$	−255.705279	−9.05	$^3IM3$	−255.766095	−47.21	$^1MoO + CO$	−255.613122	48.78
$^5IM4$	−255.705924	−9.45	$^3TS_{34}$	−255.717384	−16.64	$^1MoCO + {}^1O$	−255.421668	168.92
$^5MoO + CO$	−255.668444	14.07	$^3IM4$	−255.718205	−17.16			

reduce its energy through activation of the C–O bond. This step is exothermic by 36.14 kcal/mol, with a barrier of 2.37 kcal/mol only. $^4TS_{23}$ has a three-membered ring structure with C_s symmetry. The distance between Mo and O is shortened to 1.832 Å, and the C–O bond to 1.512 Å simultaneously. $^4TS_{23}$ is a typical early transition state, the imaginary frequency is 440.4i cm^{-1}, and the normal model corresponds to the breakage of C–O bond and the formations of Mo–O and Mo–C bonds.

Similar to insertion intermediate ^{6}IM3, there are two possible dissociation channels: The Mo–C bond rupture to form $^4MoO^+ + CO$, and the Mo–O bond cleavage to form $^3MoCO^+ + {}^3O$, which are calculated to be endothermic by 47.95 kcal/mol and 111.0 kcal/mol, respectively, so the Mo–C bond rupture is more favourable than the later.

Next let us turn to the doublet PES, as depicted in figure 2a. Similar with that of the sextet and quartet channels, the first step of the reaction over this PES is the formation of a linear encounter complex ^{2}IM1 ($^2\Sigma$, $C_{\infty v}$), exothermic by 18.46 kcal/mol, which is a barrier-free process. The C–O bond insertion intermediate ^{2}IM3 is generated by overcoming an activation barrier of 10.99 kcal/mol. ^{2}IM3 lies −7.31 kcal/mol below the ground reactants asymptote. The next step corresponds to the ^{2}IM3 →^{2}IM4 isomerization, which involves an activation barrier of 28.49 kcal/mol, and it is endothermic by 27.76 kcal/mol. From figure 1a, one can see ^{2}IM4 is a $(OMo(\eta^2CO))^+$ complex. NBO analysis shows that in ^{2}IM4, both the CO→Mo σ-donation and the effect of Mo→CO π-back-donation are very strong.

Similar to the C–O bond insertion intermediates over sextet and quartet PESs, there are two possible dissociation channels from the insertion intermediate ^{2}IM3: The Mo–C bond rupture to form $^2MoO^+ + CO$, and the Mo–O bond cleavage to form $^2MoCO^+ + {}^1O$, which are calculated to be endothermic by 45.45 kcal/mol and 204.7 kcal/mol, respectively. It is clear that the Mo–O bond rupture is more favourable than the latter. The whole reaction $^2Mo^+ + CO_2 \rightarrow {}^2MoO^+ + CO$ is calculated to be endothermic by 22.01 kcal/mol.

From the early experiment,[40] one can see that the cross section for the formation of MoO^+ is larger than $MoCO^+$, so it is clear that the dominant product of the reaction Mo^+ toward CO_2 is MoO^+, and the product MoO^+ is predicted to have ground state $^2\Delta$ from the above discussion. DFT calculations by Broclawik[54] suggest that the $^2\Delta$ state of MoO^+ may be the lowest state. Based on the B3LYP calculations, Kretzschmar *et al.*[55] also indicate the $^2\Delta$ state of MoO^+ is lower in energy than that of the $^4\Sigma$ about 7.2 kcal/mol. Whereas calculations on the CASSCF and CASPT2D level of theory suggest that the ground state is $^4\Sigma$. It appears that the above two states are close in energy. In any case, the reaction between ground state $Mo^+(^6S)$ cation and CO_2 to generate MoO^+ is spin-forbidden and has to go through intersystem crossing. From the calculation based on the B3LYP level, we can acquire the following information: (i) The ground state $^6Mo^+$ is calculated to be 32.61 kcal/mol more stable than excited state $^4Mo^+$, 60.15 kcal/mol more stable than $^2Mo^+$; (ii) The intial complex ^{6}IM1 is more stable than ^{4}IM1 by 29.61 kcal/mol, 62.45 kcal/mol more stable than ^{2}IM1; (iii) The insertion species ^{6}IM3 is less stable than ^{4}IM3 by 50.71 kcal/mol, 61.4 kcal/mol less stable than ^{2}IM3; (iv) The products $^2MoO^+ + CO$ are more stable than $^4MoO^+ + CO$ by 4.01 kcal/mol, 65.91 kcal/mol more stable than $^6MoO^+ + CO$. All these facts suggest that the formation of the MoO^+ ($^2\Sigma$) +CO($^1\Sigma$) products involves a change of spin and must therefore proceed through a crossing point of the different PESs.

From the previous experiment[40] and our calculations above, we can speculate that the intersystem crossing occur during the process of ^{6}IM1→$^4TS_{12}$, and $^4TS_{12}$ →^{2}IM3. Our following calculation is aimed at determining the region where the spin inversion occur, and acquiring the structure and energy informations of crossing point between the two different potential energy surfaces.

We choose a simple approach suggested by Yoshizawa *et al.*[56] for approximately locating the crossing points of two PESs of different multiplicities. The main idea of this approach is to perform a series of single-point computations of one spin state along the IRC of the other spin state.

Using the above method, we computed potential energy profile of the quartet state and doublet state along the sextet IRC. In figure 3a, one can see that a crossing point CP1 (between sextet and quartet PES) is before $^4TS_{12}$ with a relative energy of −255.405 Hartree. From figure 3b, another crossing point CP2 (between sextet and doublet PES) is found before $^2TS_{13}$. Obviously, along the sextet PES, as the sextet–quartet crossing taking place first, the possibility of sextet–doublet crossing is neglectable. Due to the sextet–quartet crossing taking place before sextet–doublet crossing, obviously, along the reaction coordinate, the reaction may jump from the sextet PES to the quartet one near the crossing point CP1. As can be seen from figure 3a, after passing point CP1, the quartet PES can provide a low-energy reaction pathway. Figure 3c

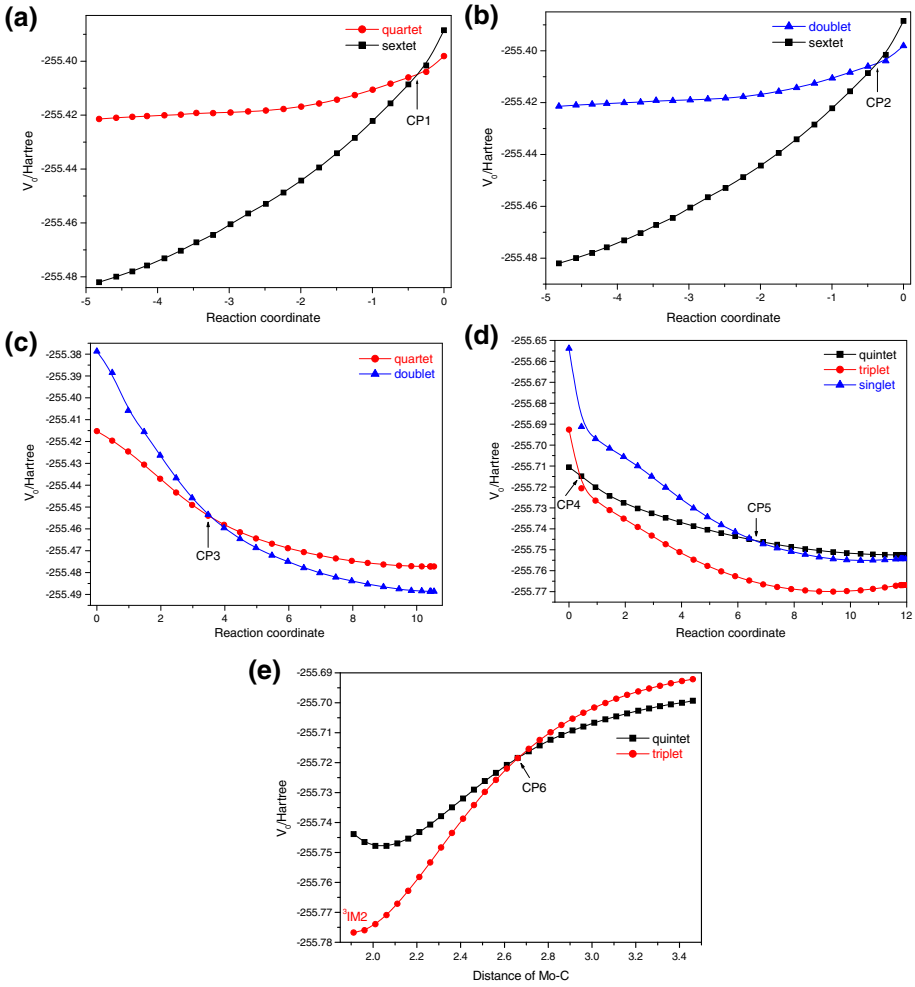

Figure 3. (**a**) Potential energies from ^{6}IM1 to ^{4}TS$_{12}$ along the sextet IRC; (**b**) Potential energies from ^{6}IM1 to ^{4}TS$_{13}$ along the sextet IRC; (**c**) Potential energies from ^{4}TS$_{12}$ to ^{2}IM3 along the quartet IRC; (**d**) Potential energies from ^{5}TS$_{23}$ to ^{3}IM3 and ^{1}IM3 along the quintet IRC; (**e**) Potential energies from ^{3}IM3 to ^{5}MoO + CO along the distance between molybdenum and carbon atom.

gives the potential energy profiles of the doublet, quartet states from the transition state ^{4}TS$_{12}$ to the insertion complex IM3 along the quartet IRC. Along the IRC we find a crossing point CP3, which is after ^{4}TS$_{12}$ with relative energy of −255.455 Hartree. Thus, the reaction may jump from the quartet PES to the doublet PES near the crossing point CP3. As a consequence, the barrier of the insertion of Mo^{+} cation into C–O bond would decrease from 79.81 kcal/mol to 66.31 kcal/mol. To conclude, the minimum energy pathway may proceed as $^{6}Mo^{+}+CO_2 \rightarrow {}^{6}$IM1$\rightarrow$CP1$\rightarrow {}^{4}TS_{12}\rightarrow$CP3$\rightarrow {}^{2}$IM3$\rightarrow {}^{2}MoO^{+}+$ CO, which is calculated to be endothermic by 38.14 kcal/mol.

Actually, the reactions catalysed by metallic systems may often involve a change in the spin states and proceed via a non-adiabatic way on two or more potential energy surfaces, denoted as 'two state reactivity' (TSR),[57–60] which has been confirmed by experimental studies. In previous theoretical researches about CO_2 activation by Nb^{+} and Zr^{+} cations, Toscano *et al.*[2,3] have ascertained the presence of some spin inversion during the reaction process, CO_2 activation mediated by metal cations was found to be an exothermic spin-forbidden process which resulted from a crossing between different energetic profiles.

3.2 *The reaction between Mo atom and CO_2*

If CO_2 approaches the ground state ^{5}Mo atom via its oxygen side, a linear encounter complex denoted as ^{5}IM1 is formed, 6.17 kcal/mol more stable than the reactants. The next step corresponds to the coordinate

between Mo and O, Mo and C atoms respectively to form a η^2–OC encounter complex ^{5}IM2 (^{5}A', C_s), which is −32.44 kcal/mol below the entrance channel ^{5}Mo + CO_2. This step only needs a low activation energy of 1.15 kcal/mol. Starting from the complex ^{5}IM2, the next step in the reaction mechanism is the insertion of the Mo atom into the C–O bond to generate ^{5}IM3. This step is endothermic by 1.22 kcal/mol and requires a high energy barrier of 25.91 kcal/mol. In ^{5}IM3, the OMo–CO binding energy is 45.29 kcal/mol which can be basically attributed to the Mo–C bond arising from a strong Mo→CO π-back-donation. This strong interaction of 4d orbital of Mo with the π-antibonding (C–O)* orbital results in the relatively long C–O bond length (1.142 Å vs 1.128 Å in free CO molecule). Further transformation of the ^{5}IM3 complex to OMo(η^2CO) (^{5}IM4) goes through the transition state called $^5TS_{34}$ with an energy barrier of 22.17 kcal/mol. ^{5}IM4 lies 9.45 kcal/mol below the reactants. NBO analysis shows that the bonding characteristics of ^{5}IM4 are different from those of ^{5}IM3. The interaction of the orbitals of Mo atom with the π-antibonding (C–O)* orbital is slight. This species can be considered as a bound complex between ^{5}MoO and CO, the dissociation of the insertion product ^{5}IM4 into ^{5}MoO + CO requires 45.29 kcal/mol energy at the UB3LYP levels.

With respect to the triplet state pathway, the first step of the reaction over this PES starts with the formation of a linear initial complex ^{3}IM1 ($^3\Sigma$, $C_{\infty v}$), 20.19 kcal/mol more stable than the reactants ^{3}Mo + CO_2. Similar with the reaction over the quintet PES, the next step corresponds to the coordinate between Nb and O, Nb and C atoms respectively to form a η^2–OC encounter complex ^{3}IM2 (^{3}A', C_s), which is −51.04 kcal/mol below the entrance channel ^{3}Mo + CO_2. Starting from ^{3}IM2, it can rearrange to form ^{3}IM3, which undergoes a rupture of C–O bond via a transition state $^3TS_{23}$ that is 13.33 kcal/mol above ^{3}IM2. As shown in figure 1b, the distance between Mo and O in $^3TS_{23}$ is shortened from 2.025 Å to 1.829 Å. This fact indicates that the weak electrostatic interaction between Mo and CO_2 strengthens when it is converted into $^3TS_{23}$, and the Mo–O bond is nearly formed. The distance between Mo and C is shortened by 0.117 Å, which suggests that the Mo–C bond is forming. At the same time, the activated C–O bond is almost broken, and the bond length is elongated by 0.328 Å. Geometrically, one can see that the $^3TS_{23}$ is similar to the η^2–OC encounter complex ^{3}IM2, so $^3TS_{23}$ is a typical 'early' transition state over the triplet PES, this is similar with the analogue ($^5TS_{23}$) over the quintet PES. The imaginary frequency of $^3TS_{23}$ is $-484.8i$ cm^{-1}, and the normal mode corresponds to the rupture of C–O bond with the result of Mo atom insertion into C–O bond. With the excess energy gained in the formation of ^{3}IM2, the cleavage process is completed smoothly.

Similar with the intermediate ^{5}IM3, there are two possible dissociation channels from ^{3}IM3: The Mo–C bond rupture to form ^{3}MoO + CO, and the Mo–O bond cleavage to form ^{3}MoCO + ^{3}O, which are calculated to be endothermic by 73.6 kcal/mol and 156.9 kcal/mol, respectively. So, it is clear that the Mo–C bond rupture is more favourable than the Mo-O bond cleavage. The whole reaction ^{3}Mo + CO_2 →^{3}MoO + CO is calculated to be exothermic by 13.34 kcal/mol. Similar to the quintet PES, we also located one (OMo(η^2CO)) complex ^{3}IM4 on this PES, which is 30.05 kcal/mol less stable than ^{3}IM3, and this isomerization process requires a relative high energy barrier of 30.57 kcal/mol.

Similar to that of the quintet and triplet channels, the first step of the reaction on the singlet path is the formation of a linear encounter complex ^{1}IM1 ($^1\Sigma$, $C_{\infty v}$), which is 60.29 kcal/mol and 34.58 kcal/mol in energy above ^{5}IM1 and ^{3}IM1 respectively. Obviously, the ground state of IM1 is in its quintet. ^{1}IM1 stores quite high energy, with reaction proceeding, this species may reduce its energy through shortening the distances between Mo and O, Mo and C atoms respectively until formation of the insertion complex ^{1}IM3. This step is exothermic (95.25 kcal/mol) with a low energy barrier of only 2.35 kcal/mol. Similar to the insertion intermediates ^{5}IM3 and ^{3}IM3, there are two possible dissociation channels from intermediate ^{1}IM3: The Mo–C bond rupture to form ^{1}MoO + CO, and the Mo–O bond cleavage to form ^{1}MoCO + ^{1}O, which are calculated to be endothermic by 89.91 kcal/mol and 210.05 kcal/mol, respectively. It is clear that the Mo–C bond rupture is more favourable than the Mo–O bond cleavage. The whole reaction ^{1}Mo + CO_2 → ^{1}MoO + CO is calculated to be exothermic by 11.37 kcal/mol. It should be pointed out that we have tried to locate the (OMo(η^2CO)) species over the singlet PES, but all our attempts failed. So, different from that of the quintet and triplet PESs, the (OMo(η^2CO)) complex may not exist over singlet one.

From the above discussion, one can see that the favourable dissociation channels from the inserted structures ^{5}IM3, ^{3}IM3 and ^{1}IM3 are the same, all of them favour to dissociate into MoO + CO.

Similar with the C–O bond activation by Mo^+ cation, the PES crossing behaviour occurs along the reaction between Mo atom and CO_2 also. On the basis of the analysis of figure 2b, several spin crossings may be

possible along the optimal reaction pathway of the C–O bond activation in CO_2 by Mo atom. First, the reaction may start with the formation of an encounter complex ^{5}IM1 on the quintet PES. Then, the quintet surface could likely cross the triplet surface somewhere between the region from $^5TS_{23}$ to ^{5}IM3. After passing the crossing point, the reaction may jump to the triplet PES since ^{3}IM3 is 6.08 and 15.99 kcal/mol below ^{1}IM3 and ^{5}IM3 respectively, i.e. the C–O bond activation complex IM3 over the triplet PES is thermodynamically more favourable than the corresponding singlet and quintet species.

Figure 3d gives the potential energy profiles of the singlet, triplet states from the complex TS_{23} to IM3 along the quintet IRC. Along the quintet IRC we find a quintet–triplet crossing point CP4, which is before ^{3}IM3 with relative energy of −255.715 Hartree. From figure 3d, one can see that the quintet-singlet crossing point CP5 lies after CP4, so this crossing is of no importance. Thus, the reaction may jump from the quintet PES to the triplet PES near the crossing point CP4 until leading to the formation of ^{3}IM3.

From above discussion, we know the energy of insertion species ^{3}IM3 is lower about 6.08 and 15.99 kcal/mol than that of the singlet and quintet analogues. But, the ground state of dissociation product MoO is in quintet. Clearly, the dissociaion process from IM3 may involve spin inversion also. Then we define the distance between Mo and C as a function, which is depicted in figure 3e. For a given Mo–C bond length, all other geometrical degrees of freedom are optimized for each spin. Along the energy curve, we find a crossing point CP6, which is at the length of Mo–C bond = 2.711 Å with relative energy of −255.716 Hartree. The structure of CP6 is presented in figure 1b. Therefore, the reaction may jump from the triplet PES to the quintet PES near the crossing point CP6. As can be seen from figure 3e, after passing point CP6, the quintet PES can provide a low-energy reaction pathway toward the dissociation products ^{5}MoO + CO.

Totally, two spin states are involved in the whole reaction, Specifically, the minimum energy pathway can be described as $^5Mo + CO_2 \rightarrow {}^5IM1 \rightarrow {}^5TS_{12} \rightarrow {}^5IM2 \rightarrow {}^5TS_{23} \rightarrow CP4 \rightarrow {}^3IM3 \rightarrow CP6 \rightarrow {}^5MoO + CO$. The whole reaction is endothermic by 14.07 kJ/mol. Obviously, compared with that of Mo^+ cation, the reaction between CO_2 and Mo atom is more active.

4. Conclusion

Density functional calculations have been performed to investigate the reactions of Mo^+ cation and Mo atom with CO_2 in gas phase. The ground and excited PESs of the titled reactions have been explored. The following conclusions can be drawn from the present calculations.

(i) The reactions of Mo^+ cation and Mo atom toward CO_2 proceed according to the insertion–elimination mechanism.
(ii) For the reaction between Mo^+ cation and CO_2, the minimum energy channel requires the crossing of three different spin states. The reactions start with the formation of a sextet encounter complex, after passing two crossing points, the reaction systems move on the doublet PES toward the products $^2MoO^+ + CO$.
(iii) For the reaction between Mo atom and CO_2, we found the reaction system would likely to change its spin multiplicity twice in going from the entrance channel to the exit channel. Specifically, it can be described as $^5Mo + CO_2 \rightarrow {}^5IM1 \rightarrow {}^5TS_{12} \rightarrow {}^5IM2 \rightarrow {}^5TS_{23} \rightarrow CP4 \rightarrow {}^3IM3 \rightarrow CP6 \rightarrow {}^5MoO + CO$.
(iv) On the doublet PES of carbon dioxide activation by Mo^+ cation, one $(OMo(\eta^2CO))^+$ complex was ensured. For the reaction between Mo atom and CO_2, the $(OMo(\eta^2CO))$ species is located both on the triplet and quintet PESs.

Acknowledgements

This work was supported by the Zhejiang Provincial Natural Science Foundation of China under grant No. Y4090387 and No. Y4100508.

References

1. Leitner W 2002 *Acc. Chem. Res.* **35** 746
2. Rondinelli F, Russo N and Toscano M 2006 *Theor. Chem. Acc.* **115** 434
3. Tommaso S D, Marino T, Rondinelli F, Russo N and Toscano M 2007 *J. Chem. Theor. Comput.* **3** 811
4. Kafafi Z H, Hauge R H, Billups W E and Margrave J L 1983 *J. Am. Chem. Soc.* **105** 3886
5. Andrews L and Tague T J 1998 *J. Am. Chem. Soc.* **120** 13230
6. Solov'ev V N, Polikarpov E V, Nemukhin A V and Sergeev G B 1999 *J. Phys. Chem. A.* **103** 6721
7. Zhou M F and Andrews L 1998 *J. Am. Chem. Soc.* **120** 13230
8. Galan F, Fouassier M, Tranquille M, Mascetti J and Papai I 1997 *J. Phys. Chem. A.* **101** 2626
9. Chertihin G V and Andrews L 1995 *J. Am. Chem. Soc.* **117** 1595
10. Zhou M F and Andrews L 1999 *J. Phys. Chem. A.* **103** 2066

11. Sievers M R and Armentrout P B 1999 *Int. J. Mass. Spectrom.* **185** 117
12. Sievers M R and Armentrout P B 1998 *Int. J. Mass. Spectrom.* **179** 115
13. Sievers M R and Armentrout P B 1999 *Inorg. Chem.* **38** 397
14. Sievers M R and Armentrout P B 1995 *J. Chem. Phys.* **102** 754
15. Sievers M R and Armentrout P B 1998 *Int. J. Mass. Spectrom.* **179** 103
16. Kretzschmar I, Schroder D, Schwarz H and Armentrout P B 2006 *Int. J. Mass. Spectrom.* **249** 263
17. Chen M, Wang X, Zhang L and Qin Q Z 2000 *J. Phys. Chem. A.* **104** 7010
18. Souter P F and Andrews L 1997 *Chem. Commun.* 777
19. Wang X, Chen M, Zhang L and Qin Q Z 2000 *J. Phys. Chem. A.* **104** 758
20. Souter P F and Andrews L 1997 *J. Am. Chem. Soc.* **119** 7350
21. Zhou M F, Liang B and Andrews L 1999 *J. Phys. Chem. A.* **103** 2013
22. Liang B and Andrews L 2002 *J. Phys. Chem. A.* **106** 595
23. Liang B and Andrews L 2002 *J. Phys. Chem. A.* **106** 4042
24. Andrews L, Zhou M F, Liang B, Li J and Bursten B E 2000 *J. Am. Chem. Soc.* **122** 11440
25. Quere A M L, Xu C and Manceron L 1991 *J. Phys. Chem.* **95** 3031
26. Papai I, Schubert G, Hannachi Y and Mascetti J 2002 *J. Phys. Chem. A.* **106** 9551
27. Papai I, Mascetti J and Fournier R 1997 *J. Phys. Chem. A.* **101** 4465
28. Papai I, Hannachi Y, Gwizdala S and Mascetti J 2002 *J. Phys. Chem. A.* **106** 4181
29. Hannachi Y, Mascetti J, Stirling A and Papai I 2003 *J. Phys. Chem. A.* **107** 6708
30. Dobrogorskaya Y, Mascetti J, Papai I and Hannachi Y 2005 *J. Phys. Chem. A.* **109** 7932
31. Zhou M F, Tsumori N, Li Z, Fan K N, Andrews L and Xu Q 2002 *J. Am. Chem. Soc.* **124** 12936
32. Jiang L and Xu Q 2005 *J. Am. Chem. Soc.* **127** 42
33. Xu Q, Jiang L and Tsumori N 2005 *Angew. Chem. Int. Ed.* **44** 4338
34. Jiang L and Xu Q 2005 *J. Am. Chem. Soc.* **127** 8906
35. Campbell M L 1999 *Phys. Chem. Chem. Phys.* **1** 3731
36. Campbell M L 2000 *Chem. Phys. Lett.* **330** 547
37. Yrsson R and Mascetti J 2005 *React. Kinet. Catal. Lett.* **285** 107
38. Jiang L, Zhang X B, Han S and Xu Q 2008 *Inorg. Chem.* **47** 4826
39. Jiang L and Xu Q 2007 *J. Phys. Chem. A.* **111** 3519
40. Sievers M R and Armentrout P B 1998 *J. Phys. Chem. A.* **102** 10754
41. Fischer G, Goursot A, Coq Bernard, Delahay G and Pal S 2006 *ChemPhysChem.* **7** 1795
42. Cho H G and Andrews L 2005 *J. Am. Chem. Soc.* **127** 8226
43. Armentrout P B 2007 *Organometallics.* **26** 5473
44. Armentrout P B 2007 *Organometallics.* **26** 5486
45. Rutkowska-Zbik D, Tokarz-Sobieraj R and Witko M 2007 *J. Chem. Theor. Comput.* **3** 914
46. Becke A D 1993 *J. Chem. Phys.* **98** 5648
47. Lee C, Yang W and Parr R G 1988 *Phys. Rev. B.* **37** 785
48. Holthausen M C and Koch W 1996 *J. Am. Chem. Soc.* **118** 9932
49. Holthausen M C, Fiedler A, Schwarz H and Koch W 1996 *J. Phys. Chem.* **100** 6236
50. Guo Z, Ke Z F, Phillips D L and Zhao C Y 2008 *Organometallics.* **27** 181
51. Dolg M, Stoll H, Savin A and Preuss H 1989 *Theor. Chim. Acta.* **75** 173
52. Fukui K 1981 *Accounts. Chem. Res.* **14** 363
53. Frisch M J, Trucks G W, Schlegel H B, Scuseria G E, Robb M A, Cheeseman J R, Zakrzewski V G, Montgomery J A Jr, Stratmann R E, Burant J C, Dapprich S, Millam J M, Daniels A D, Kudin K N, Strain M C, Farkas O, Tomasi J, Barone V, Cossi M, Cammi R, Mennucci B, Pomelli C, Adamo C, Clifford S, Ochterski J, Petersson G A, Ayala P Y, Cui Q, Morokuma K, Malick D K, Rabuck A D, Raghavachari K, Foresman J B, Cioslowski J, Ortiz J V, Baboul A G, Stefanov B B, Liu G, Liashenko A, Piskorz P, Komaromi I, Gomperts R, Martin R L, Fox D J, Keith T, Al-Laham M A, Peng C Y, Nanayakkara A, Gonzalez C, Challacombe M, Gill P M W, Johnson B, Chen W, Wong M W, Andres J L, Gonzalez C, Head-Gordon M, Replogle E S and Pople J A 2003 Gaussian 03, Revision B04, Pittsburgh PA: Gaussian Inc.
54. Broclawik E 1995 *Int. J. Quantum. Chem.* **56** 779
55. Kretzschmar I, Fiedler A, Harvey J N, Schroder D and Schwarz H 1997 *J. Phys. Chem. A.* **101** 6252
56. Yoshizawa K, Shiota Y and Yamabe T 1999 *J. Chem. Phys.* **111** 538
57. Fiedler A, Schroder D, Shaik S and Schwarz H 1994 *J. Am. Chem. Soc.* **116** 3563
58. Harvey J N, Poli R and Smith K M 2003 *Coord. Chem. Rev.* **238** 347
59. Zhang G B, Li S H and Jiang Y S 2003 *Organometallics.* **22** 3820
60. Schroder D, Shaik S and Schwarz H 2000 *Acc. Chem. Res.* **33** 139